A Quantum Annealer for Subset Feature Selection and the Classification of Hyperspectral Images

Soronzonbold Otgonbaatar and Mihai Datcu, *Fellow, IEEE*

***Abstract*—Hyperspectral images (HSIs) showing objects belonging to several distinct target classes are characterized by dozens of spectral bands being available. However, some of these spectral bands are redundant and/or noisy, and hence, selecting highly informative and trustworthy bands for each class is a vital step for classification and for saving internal storage space; then the selected bands are termed a highly informative spectral band subset. We use a mutual information (MI)-based method to select the spectral band subset of a given class and two additional binary quantum classifiers, namely a quantum boost (Qboost) and a quantum boost plus (Qboost-Plus) classifier, to classify a two-label dataset characterized by the selected band subset. We pose both our MI-based band subset selection problem and the binary quantum classifiers as a quadratic unconstrained binary optimization (QUBO) problem. Such a quadratic problem is solvable with the help of conventional optimization techniques. However, the QUBO problem is an NP-hard global optimization problem, and hence, it is worthwhile for applying a quantum annealer. Thus, we adapted our MI-based optimization problem for selecting highly informative bands for each class of a given HSI to be run on a D-Wave quantum annealer. After the selection of these highly informative bands for each class, we employ our binary quantum classifiers to a two-label dataset on the D-Wave quantum annealer. In addition, we provide a novel multilabel classifier exploiting an error-encoding output code when using our binary quantum classifiers. As a real-world dataset in Earth observation, we used the well-known AVIRIS HSI of Indian Pine, north-western Indiana, USA. We can demonstrate that the MI-based band subset selection problem can be run on a D-Wave quantum annealer that selects the highly informative spectral band subset for each target class in the Indian Pine HSI. We can also prove that our binary quantum classifiers and our novel multilabel classifier generate a correct two- and multilabel dataset characterized by their selected bands and with high accuracy such as having been produced by conventional classifiers—and even better in some instances.**

***Index Terms*—D-wave quantum annealer (QA), feature selection, hyperspectral images (HSIs), mutual information (MI), quantum machine learning, quantum classifier.**

Manuscript received March 4, 2021; revised May 21, 2021; accepted June 27, 2021. Date of publication July 7, 2021; date of current version July 23, 2021. This work was supported by the Juelich Supercomputing Centre (https://www.fzjuelich.de/ias/jsc) by providing computing time through the Juelich UNified Infrastructure for Quantum computing (JUNIQ) on a D-Wave QA. *(Corresponding author: Soronzonbold Otgonbaatar.)*

Soronzonbold Otgonbaatar is with the German Aerospace Center (DLR), 82234 Wessling, Germany, and also with the University of Siegen, 57076 Siegen, Germany (e-mail: soronzonbold.otgonbaatar@dlr.de).

Mihai Datcu is with the German Aerospace Center (DLR), 82234 Wessling, Germany, and also with University POLITEHNICA of Bucharest (UPB), 060042 Bucharest, Romania (e-mail: mihai.datcu@dlr.de).

Digital Object Identifier 10.1109/JSTARS.2021.3095377

I. Introduction

A QUANTUM annealer (QA) is a computing machine configured as a graph network $G = (E, V)$, at each vertex of which particles are residing, and its edges define the interaction strengths among these particles, which are in quantum states ups or $downs$. For a D-Wave QA, the graph G has a specific network topology named *Pegasus*, in which only certain edges are connected. In particular, the interaction among the particles is constrained [1], [2].

A D-Wave QA works as a metaheuristic process, which is dedicated to tackle specific classes of optimization problems, e.g., quadratic unconstrained binary optimization (QUBO) problems. There are theoretical studies that a D-Wave QA can solve these QUBO problems faster than a conventional annealer (even for NP problems) [3], [4]. However, currently, there are no indications of computational advantages for real-world problems. For practical applications, several studies are devoted to benchmark and assess a D-Wave QA for an operational planning and feature extraction from remotely sensed images [5], [6].

For a real-world dataset in Earth observation, remotely sensed images differ in their image content representations due to the diverse satellite platforms with their different types of sensors. When we want to use a D-Wave QA with an Earth observation dataset, some of the challenges are the proper choice of appropriate remotely sensed images specified by their image content representations such as their spatial information, polarization states, spectral bands, and the embedding of a given dataset in the topology of a D-Wave QA. Here, we consider hyperspectral images (HSIs), and a selection of their highly informative band subset is a very vital procedure in Earth observation. Hence, we use a mutual information (MI)-based optimization method to select the highly informative band subset, and more importantly, we can easily embed and optimize the MI-based optimization method in the *Pegasus* topology of a D-Wave QA. Therefore, HSIs are one of the most proper datasets in Earth observation for a D-Wave QA than others. In particular, HSIs became an important field of study to classify or identify objects in a ground scene such as roads, land cover, or agriculture since each object is characterized by a high-dimensional vector of the different spectral bands within the given full wavelength range. Due to the rich information content of the spectral bands, some of these bands carry more discriminatory information than others. Hence, some studies are focused on extracting highly informative features or a dimensionality reduction of HSIs, for instance, by using deep learning networks or principal component analysis

(PCA) [7], [8]. On the other hand, some researchers focused on how to select a highly informative band subset by using the concept of the information theory; in particular, MI-based methods that provide a measure of independence between several spectral bands. Moreover, these MI-based methods are based on prior or reference knowledge of the spectral signatures of objects; such knowledge can be obtained in specific spectral-signature databases of common ground targets [9], [10].

In this article, we use an Indian Pine HSI of Indian Pine composed of $l = 16$ distinct classes. Each class is characterized by $n = 200$ bands (features); thus, the number of subsets of the features of a given class, e.g., $y_S = 1$, is 2^n combinations. A way to find the best feature subset of this given class is to try all combinations. This is clearly computationally expensive for a large number of these features.

Hence, in the first part of this study, we introduce an MI-based subset feature selection problem as a global optimization problem for the Indian Pine HSI. Then, we propose to optimize this MI-based band subset selection problem on a D-Wave QA. As a first step, we map the MI-based band subset selection problem to a QUBO-based band subset selection problem. This is our first *problem mapping* step. Second, we optimize this mapping problem on a D-Wave QA; *quantum optimization* [11], [12]; this part was strongly motivated by a feature selection tutorial offered by D-Wave [2].

In the second part of this study, we use binary quantum classifiers, namely a quantum boost (Qboost) and a quantum boost plus (Qboost-Plus) classifier, in contrast to an adaptive boost (Adaboost) classifier [13], [14]. We first apply these quantum classifiers to a two-label dataset of the Indian Pine HSI, and second, we provide a novel multilabel classifier via an error-encoding output code (ECOC) when using our binary quantum classifiers [15], [16]; each resulting class is discriminated by the selected bands in the first part of our study. We also benchmarked and assessed these binary quantum classifiers and the novel multilabel classifier with respect to conventional classifiers, a decision tree classifier (DTC), a support vector machine (SVM), and an Adaboost classifier.

Our contribution in this article is then an attempt to benchmark and assess a D-Wave QA for Earth observation data and to recognize the challenges that are encountered with real-world datasets and future QAs or devices. Toward these goals, we are employing a D-Wave QA for feature selection and classification of the Indian Pine HSI as a machine learning technique; our contribution consists of a three-step approach.

1) Feature selection on a D-Wave QA: The MI-based band subset selection.
2) Binary classification on a D-Wave QA: The binary quantum classifiers to a two-label dataset characterized by those selected bands.
3) Multi-label classification on a D-Wave QA: The ECOC generates a multilabel dataset when we are using our binary quantum classifiers.

Moreover, the D-Wave QA may prove relevant even if we are not intending to demonstrate its advantage over a conventional annealer.

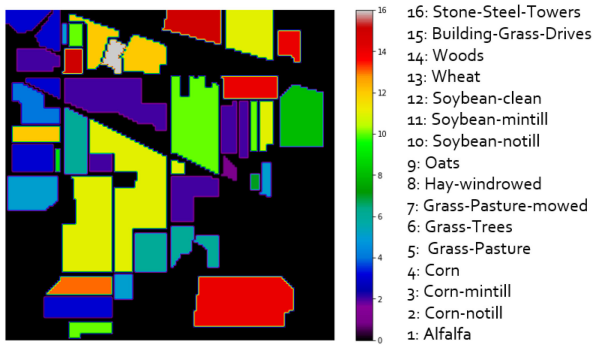

Fig. 1. Indian Pine HSI: Ground truth.

This article is structured as follows. We introduce the basics of hyperspectral imaging in Section II. We present the basics of the information theory and MI-based band subset selection problem in Section III. In Section IV, we discuss the fundamentals of a QUBO problem and demonstrate the *problem mapping* of an MI-based problem to a QUBO-based problem. We introduce the basics of a D-Wave QA and optimize the QUBO-based band subset selection problem for the Indian Pine HSI on a D-Wave QA (see Section V, *quantum optimization*). Finally, we apply the binary quantum classifiers and the novel multilabel classifier to the two- and multilabel dataset in Sections VI, and VII, respectively. Section VIII concludes this article.

II. Introduction to Hyperspectral Imaging

A hyperspectral imaging sensor mounted on a satellite or aircraft measures the electromagnetic spectrum ranging from the visible to the near infrared wavelengths; for instance, the imaging spectroscopy and the airborne visible/infrared imaging spectrometer (AVIRIS) sensor measures 224 continuous spectral bands ranging from 400 to 2500 nm at 10-nm intervals [17].

As a real-world dataset of HSIs, we consider an Indian Pine HSI obtained by the AVIRIS sensor (see Fig. 1). This low-noise Indian Pine image having the spectral bands of $X = \{\text{band1}, \ldots, \text{band200}\}$ elements is a high-dimensional dataset. However, not all of these spectral bands are informative for characterizing a specific class; in other words, some bands of X are redundant or noisy.

It is advantageous to select a highly informative band subset of the given spectral bands for a given class. Hence, we employ an MI-based band subset selection problem as a global optimization problem.

III. Information Theory and MI-Based Band Subset Selection

We select a highly informative band subset for each class of the Indian Pine HSI; for instance, we consider the spectral bands $X = \{X_1, \ldots, X_{200}\} = \{\text{band1}, \ldots, \text{band200}\}$ of a given class y_S and find its most informative band subset. To find the highly informative band subset for that specific class, we employ an information theory; information is a function of probabilities. Hence, we represent the band X_i and its corresponding class y_S as probabilities. We derived the probabilities

for the band X_i and its class y_S by dividing them into ten bins in a histogram. The probability is then defined as

$$P(X_{n'}) = \frac{X_{n'}}{\sum_{n'=1}^{10} X_{n'}}, \quad P(y_{m'}) = \frac{y_{m'}}{\sum_{m'=1}^{10} y_{m'}} \tag{1}$$

where $X_{n'}$ and $y_{m'}$ represent the number of occurrences of the band X_i and its class y_S in the n'th or m'th bin, respectively. Their joint probability is defined in the same way.

For the selection of the band subset, we exploit *mutual information (MI)* that measures independence between band X_i and its class y_S. It is defined by

$$I(X_i; y_S) = \sum_{m'} \sum_{n'} P(X_{n'}, y_{m'}) \log \frac{P(X_{n'}, y_{m'})}{P(X_{n'})P(y_{m'})} \tag{2}$$

and by *conditional mutual information (CMI),* which is a measure of the dependence between the band X_i and its class y_S given another band X_j. The CMI can then be written as

$$I(X_i; y_S|X_j) = E(X_i|X_j) - E(X_i|y_S, X_j) \tag{3}$$

where E is the entropy that is a measure of the uncertainty of a random variable [18].

These band subset selection techniques expressed by both (2) and (3) are named after an *MI-based band subset selection* problem, which became popular in machine learning due to its strong mathematical foundation rooted in the information theory.

In the next sections, we pose the MI-based band subset selection problem as a global optimization problem. First, we map our MI-based band subset selection problem to a QUBO problem, and the QUBO problem to a QUBO-based band subset selection problem. Finally, we optimize the QUBO-based band subset selection problem on a D-Wave QA.

IV. Problem Mapping: The QUBO-Based Band Subset Selection

A. Mapping of a MI-Based Problem to a QUBO Problem

In this part, we consider and pose the MI-based band subset selection problem as a global optimization problem [11], [12]. Moreover, the maximization over the subsets $\{X_i\}$ can be written as

$$\max_{\{X_i\}} \left[\sum_{X_i} I(X_i; y_S) + \sum_{X_i, X_j} I(X_i; y_S|X_j) \right] \tag{4}$$

where X_i represents the bands of a given class y_S of the Indian Pine HSI (see Fig. 1).

Let us consider the band data $X = \{band1, \ldots, band200\}$ of a given class of *Alfalfa* or simply $y_S = 1$ as an example case. We assume that (4) is maximized when we use the subset $X_S = \{X_1, X_2\} = \{band1, band2\}$. We can express this result in a matrix form such that

$$I(X_1; y_S) + I(X_1; y_S|X_2) + I(X_2; y_S) + I(X_2; y_S|X_1) \Leftrightarrow$$
$$\Leftrightarrow \begin{pmatrix} \tilde{x}_1 & \tilde{x}_2 \end{pmatrix} \begin{pmatrix} I(X_1; y_S) & I(X_1; y_S|X_2) \\ I(X_2; y_S|X_1) & I(X_2; y_S) \end{pmatrix} \begin{pmatrix} \tilde{x}_1 \\ \tilde{x}_2 \end{pmatrix} \tag{5}$$

here, $\tilde{x}_1 = 1$, $\tilde{x}_2 = 1$, and $\tilde{x}_3 = \cdots = \tilde{x}_n = 0$. On the other hand, we can interpret this matrix form that the $\tilde{x}_n$'s are for selecting a highly informative band subset. Hence, we can express the MI-maximization problem expressed by (4) alternatively as

$$\max_{\vec{x}} [\vec{x}^T Q \vec{x}], \quad \vec{x} = (\tilde{x}_1, \tilde{x}_2, \ldots, \tilde{x}_n)^T, \quad \vec{x} \in \{0, +1\}^n \tag{6}$$

where T represents a transpose operation, and Q is represented diagonal $Q_{ii} = I(X_i; y_S)$ and off-diagonal $Q_{ij} = I(X_i; y_S|X_j)$ elements. We can even transform this maximization problem to a minimization problem by multiplying it by "-1." As a result, we have

$$\min_{\vec{x}} [\vec{x}^T Q \vec{x}], \quad \vec{x} \in \{0, +1\}^n \tag{7}$$

where $Q_{ii} = -I(X_i; y_S)$ and $Q_{ij} = -I(X_i; y_S|X_j)$ [11]. This form of the minimization problem over binary variables $\vec{x}$ is called a QUBO problem.

The MI-based band subset selection problem is, therefore, equivalent to a QUBO problem when we write "$-I(X_i; y_S)$" and "$-I(X_i; y_S|X_j)$" in the Q matrix, and minimize the Q matrix over the binary variables.

B. Mapping the QUBO Problem to the QUBO-Based Subset Band Selection Problem

To select a highly informative band subset characterizing each class of the Indian Pine image (see Fig. 1), we employ the QUBO problem described by (7) with an additional constraint

$$\min_{\vec{x}} [\vec{x}^T Q \vec{x}], \quad s.t. \quad \sum_{i=1}^{n} \tilde{x}_i = k, \quad \tilde{x}_i \in \{0, +1\} \tag{8}$$

where k is the number of bands (band subset) of interest, and $n = 200$ is the total number of given bands. Hence, we define the QUBO-based band subset selection problem as

$$\min_{\vec{x}} \left[\vec{x}^T Q \vec{x} + \gamma \sum_{i=1}^{n} (\tilde{x}_i - k)^2 \right], \quad \vec{x} \in \{0, +1\}^n \tag{9}$$

where γ is a Lagrange multiplier. As an experiment for selecting the most informative band subset for the specific class of an Indian Pine HSI, we consider the band subsets with three elements $(k = 3)$.

V. Quantum Optimization: Using a D-Wave QA

A. D-Wave QA

We selected a highly informative band subset characterizing the specific class of the Indian Pine HSI by optimizing the QUBO-based band subset selection problem in the form of (9). We optimized this optimization problem on a D-Wave QA, and we even benchmark the D-Wave QA with respect to its conventional version.

A D-Wave QA is a QA for the special class of optimization problems, in particular, QUBO-like problems. Such a QA is a metaheuristic process evolving slowly enough from its initial energy H_i to its final energy H_f in the form of a QUBO problem. The evolution process is expressed by

$$H(t) = (1 - \lambda(t))H_i(\hat{X}) + \lambda(t)H_f(\hat{Z}) \tag{10}$$

Algorithm 1: Fitting Weak Classifiers.

INPUT: Training bands:
$(\mathbf{x}, \mathbf{y}) = (x_1, y_1), \ldots, (x_S, y_S)$; $\triangleright x_S$ represents the three selected bands for a given class y_S (see Table I).
$\mathbf{y} \in \{-1, +1\}^S$; $\triangleright S$ is the size of the input dataset, and $\mathbf{y}$ represents the two-label of the Indian Pine HSI (see Table III).
Initialize the weak classifiers: $c = [c_1, \ldots, c_N]$; $\triangleright$DTCs.
N; $\triangleright$the number of DTCs.
$w_S = (1, \ldots, 1)/S$; $\triangleright$Assigning the same weight to each data element x_S.
for $i \leftarrow 1, \ldots, N$ **do**
  Fit a DTC, $c[i]$, to the $(\mathbf{x}, \mathbf{y})$ with a weight w_S.
  $\mathbf{y}_p = c[i](\mathbf{x}), \quad \mathbf{y}_p \in \{-1, +1\}^S$.
  $err_m = w_S \cdot \mathbb{I}(\mathbf{y}_p ! = \mathbf{y})/\text{sum}(w_S)$.
  $a_m = 0.5 \cdot \log \dfrac{1 - \text{err}_m}{\text{err}_m}$.
  $w_S = w_S \cdot \exp(-a_m \cdot \mathbf{y}_p \cdot \mathbf{y})$; $\triangleright$boosting the weight of misclassified data.
  $w_S = w_S/\text{sum}(w_S)$.
end for
$h = [h_1, \ldots, h_N], \quad h_n \in \mathbb{R}^S$; $\triangleright$defining an array to store the weak classifier predictions.
for $i \leftarrow 1, \ldots, N$ **do**
  $h[i] = c[i](\mathbf{x})$; $\triangleright$storing the predicted classes.
end for
$h = h/N$; $\triangleright$scaling h to the range of $[-1/N, 1/N]$.
return h.
STOP ALGORITHM.

TABLE I
SELECTION OF THE BEST BAND SUBSET FOR EACH CLASS OF THE INDIAN PINE HSI BY USING THE QUBO-BASED BAND SUBSET SELECTION ON A D-WAVE QA

Class labels Y	Selected Bands X_i		
Alfalfa	band41	band47	band77
Corn-notill	band13	band15	band17
Corn-mintill	band3	band133	band190
Corn	band49	band128	band175
Grass-Pasture	band102	band143	band84
Grass-Trees	band23	band40	band53
Grass-Pasture-mowed	band61	band102	band109
Hay-windrowed	band149	band150	band40
Oats	band76	band85	band172
Soybean-notill	band10	band145	band183
Soybean-mintill	band12	band145	band180
Soybean-clean	band4	band12	band136
Wheat	band37	band82	band177
Wood	band63	band102	band190
Building-Grass-Drives	band18	band70	band109
Stone-Steel-Towers	band79	band84	band104

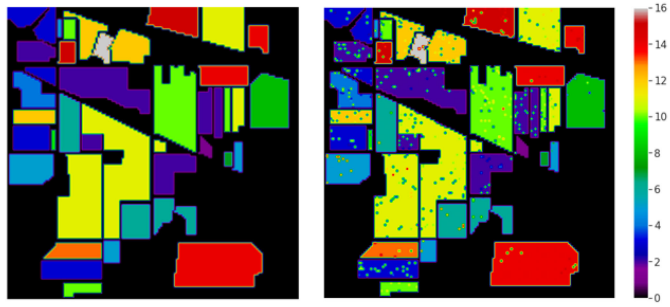

Fig. 2. (Left) Ground truth. (Right) Classification of the $l = 16$ classes characterized by three highly informative spectral bands shown in Table I by using an SVM.

where $\hat{X}$ and $\hat{Z}$ are Pauli-x and $-z$ matrices, H_i is the initial Hamiltonian of a system for a given time function of $\lambda(t) = 0$, and H_f is the QUBO problem with $\lambda(t) = 1$ [1]–[3].

The hardware of the D-Wave QA has a specific graph topology $G = (V, E)$ named *Pegasus*; its vertices represent binary variables $\vec{x}$, and its edges define interaction strengths among the binary variables. However, the connectivity of these binary variables in the *Pegasus* topology is very constrained; in particular, only the certain binary variables are allowed to interact with others through the edges [19].

In addition, the performance of a D-Wave QA strongly depends on mapping the binary variables of our QUBO problem expressed by (9) to the Pegasus topology. As it is possible to map (embed) our QUBO problem to the Pegasus topology as efficiently as possible, we employed a technique called *minor embedding*, which is offered by the company D-Wave systems [2], [19].

B. Quantum Optimization for the Band Subset Selection

Quantum optimization is an optimization of our QUBO-based band subset selection problem on a D-Wave QA. We performed our experiment in a classical annealer and a D-Wave QA. Both of these annealers selected the same band subset for each class of the Indian Pine HSI; we shown these selected band subsets in Table I, while $k = 3$ in (9).

To prove that we selected the highly informative band subset for each class on a D-Wave QA, we performed the scene classification for our Indian Pine HSI by using a DTC and an SVM shown in Fig. 2 as a proof-of-concept.

In addition, we discovered that we needed at least a 10-D parameter to reach the same accuracy as our proof-of-concept method when we apply the PCA for the dimensionality reduction and conventional classifiers (the DT and the SVM) for the multiclass classification of the Indian Pine HSI (see Table I) [8]. For this scenario, we present the classification accuracy of the test dataset in Table II.

These findings lead to the conclusion that our QUBO-based band subset selection method identified the highly informative band subset, and it even helped to reduce a storage space and the computational load for training the given classifiers.

VI. CASE STUDY OF A BINARY QUANTUM CLASSIFIER ON A D-WAVE QA FOR HSI

We have the Indian Pine HSI with 16 classes, where each class is characterized by three highly informative bands selected by our QUBO-based band subset selection method shown in

Algorithm 2: Qboost Classifier.

INPUT: h from (Algorithm 1) or given.
OUTPUT: The strong classifier C.
Fit the weak classifiers to $(\mathbf{x}, \mathbf{y})$ (Algorithm 1): h (if h is not given).
The weak subset classifier selection:
$\alpha^* = \min_\alpha[\alpha^T Q \alpha], \quad \alpha \in \{0, +1\}^N$; ▷QUBO problem
Diagonal and off-diagonal elements of a matrix Q:
$Q \in \mathbf{R}^{N \times N}$.
for $i \leftarrow 1, \ldots, N$ **do**
  $Q_{ii} = S/N^2 + \lambda - 2(h[i])^T \cdot \mathbf{y}$.
end for
for $i \leftarrow 1, \ldots, N$ **do**
  for $j \leftarrow i + 1, \ldots, N$ **do**
    $Q_{ij} = (h[i])^T \cdot h[j]$.
  end for
end for
Optimize QUBO problem on a D-Wave QA
An optimal estimator weight vector: α^*.
PREDICT: given the test band set $(x_1, \ldots x_t)$;
$T = \frac{1}{t} \sum_{t=1}^{t} \sum_{i=1}^{N} \alpha^* h[i](x_t)$.
$C(x_t) = sign(\sum_{i=1}^{N} \alpha^*[i] h[i](x_t) - T)$.
STOP ALGORITHM.

TABLE II
CLASSIFICATION ACCURACY OF THE DTC AND THE SVM

QUBO-based band selection			PCA	
Classifier	DTC	SVM	DTC	SVM
Accuracy	0.74	0.81	0.72	0.81

Table I. In this section, we analyze binary quantum classifiers, namely a Qboost classifier, and a Qboost-Plus classifier, for a two-label dataset of the Indian Pine HSI created as the binary output of a D-Wave QA; for instance, *Alfalfa and Corn-notill*, or *Corn-mintill and Corn-notill*, etc. Further, we benchmarked the classification accuracy of our binary quantum classifiers with respect to conventional binary classifiers, such as a DTC, an SVM, and an Adaboost classifier.

We considered first two types of boosting algorithms, a Qboost and an Adaboost algorithm (classifier). The Qboost classifier is a quantum version of an Adaboost classifier. Here, we use two types of terminology for these classifiers, a strong classifier C and a weak classifier c_i. The strong classifier leverages many weak classifiers to achieve its high classification accuracy; the weak classifier is a classifier that classifies a given dataset better than random guessing [20].

A. Basics of an Adaboost Classifier

An Adaboost classifier is an algorithm for finding an optimal estimator weight of many weak classifiers so that the classifier C is maximized [21]

$$C(x_S) = \text{sign}\left[\sum_{i=1}^{N} \alpha_i c_i(x_S)\right], \quad c_i(x_S) \in \{-1, +1\} \quad (11)$$

where (x_S, y_S) represents a training dataset, and $\alpha_i \in [0, +1]$ is the estimator weight that is continuous-valued. Here, $\text{sign}(f(x_S)) = 1$ if $f(x_S) > 0$, $\text{sign}(f(x_S)) = -1$ if $f(x_S) < 0$, and $\text{sign}(f(x_S)) = 0$ otherwise. The loss of the Adaboost classifier is defined as an exponential loss

$$\boldsymbol{\alpha}^* = \min_{\boldsymbol{\alpha}} \left[\sum_{s=1}^{S} \exp -y_s \sum_{i=1}^{N} \alpha_i c_i(x_s)/S\right]. \quad (12)$$

In contrast, a Qboost classifier is an algorithm for finding an optimal estimator weight that takes only binary numbers $\alpha_i \in \{0, +1\}$, and its loss is defined by a squared loss denoted as L_2. Hence, the Qboost classifier is equivalent to a subset selection algorithm among many weak classifiers to approximately maximize the accuracy of the strong classifier. In next section, we delve into the Qboost classifier in more detail.

In general, these boosting algorithms start with assigning identical weights w_S to our dataset. The weak classifiers classify these datasets, and if the data are misclassified, then the weight of that data are increased (boosted). This procedure is repeated until no further improvement in the classification accuracy can be seen. A DTC with a depth of one is considered as a weak classifier; sometimes, it is called a decision stump classifier. We already presented the steps for boosting a weight w_S and the weak classifier in Algorithm 1.

B. Qboost Classifier for a Two-Label Dataset of the Indian Pine HSI

Moving toward the Qboost classifier, after having stopped boosting the weight of our dataset, the Qboost classifier selects the weak subset classifier so that the classification accuracy of the strong classifier is maximized. We executed the weak subset classifier selection algorithm on a D-Wave QA as shown in Algorithm 2. Below, we explain the derivation of Algorithm 2 in detail. More importantly, the Qboost classifier exploits the weight boosting by solving the weak subset classifier selection problem on a D-Wave QA.

For the two-label dataset of the Indian Pine HSI, we define the training band dataset as $(x_1, y_1), \ldots, (x_S, y_S)$, the test band dataset as $(x_1, \ldots, x_t)$, and the strong classifier, $C(x_S) \in \{-1, +1\}$, which is a binary classifier in the form of [13] and [20]

$$C(x_S) = \text{sign}\left[\sum_{i=1}^{N} \alpha_i c_i(x_S)\right], \quad c_i(x_S) \in \{-1, +1\} \quad (13)$$

where $\alpha_i \in \{0, 1\}$ is the estimator weight, and $c_i(x_S)$ is the weak classifier; we chose DTCs as our weak classifiers.

Recent papers on theoretical studies [13], [14] and a practical application for the remote sensing [22] are proposed to formulate the loss of the strong classifier as a squared loss L_2

$$\alpha^* = \min_{\alpha_i, \lambda} \left[\sum_{s=1}^{S} \left(\sum_{i=1}^{N} \alpha_i c_i(x_s) - y(x_s)\right)^2 + \lambda \sum_{i=1}^{N} \alpha_i^0\right] \quad (14)$$

where α^* represents the optimal estimator weight vector, S is the size of the training band dataset, and $\lambda \sum_{i=1}^{N} \alpha_i^0$ represents a

0-norm term. By expanding the squared loss function, we have

$$\alpha^* = \min_{\alpha,\lambda} \left[\sum_{i=1}^{N} \sum_{j=1}^{N} \alpha_i \alpha_j \left(\sum_{s=1}^{S} c_i(x_s) c_j(x_s) \right) + \sum_{i=1}^{N} \alpha_i \left(\lambda - 2 \sum_{s=1}^{S} c_i(x_s) y(x_s) \right) \right] \tag{15}$$

which is in the form of a QUBO problem, while we define

$$\begin{aligned} Q_{ij} &= \sum_{s=1}^{S} c_i(x_s) c_j(x_s) \\ Q_{ii} &= S/N^2 + \lambda - 2 \sum_{i=1}^{N} c_i(x_S) y(x_S). \end{aligned} \tag{16}$$

Then, we can write

$$\alpha^* = \min_{\alpha} [\alpha^T Q \alpha], \quad \alpha \in \{0, +1\}^N. \tag{17}$$

We optimized this problem on a D-Wave QA to select the weak subset classifier in its quadratic form.

Then, we obtained the optimal estimator weight vector α^*, and the strong classifier for the test band dataset becomes

$$\begin{aligned} C(x_t) &= \text{sign} \left[\sum_{i=1}^{N} \alpha_i^* c_i(x_t) - T \right] \\ T &= \frac{1}{t} \sum_{t=1}^{t} \sum_{i=1}^{N} \alpha^* c_i(x_t) \end{aligned} \tag{18}$$

where $(x_1, \ldots x_t)$ are from the test band dataset of the Indian Pine HSI, and T is derived experimentally to increase the classification accuracy of the strong classifier $C(x_t)$ [13], [14]. We have already presented the procedures of the Qboost classifier in Algorithms 1 and 2.

Second, we chose the *DTC*, *SVM*, and *Qboost* classifiers as weak classifiers instead of only a DTC. This method is sometimes called an ensemble method. By exploiting (13) and (15), we again formulated weak classifiers such that

$$C(x_S) = \text{sign} \left[\sum_{i=1}^{3} \alpha_i c_i(x_S) \right], \quad c_i(x_S) \in \{-1, +1\} \tag{19}$$

where $c_1(x_S)$, $c_2(x_S)$, and $c_3(x_S)$ represent the *DTC*, *SVM*, and *Qboost* classifiers, respectively. In this scenario, we have $h = [c_1(x_S), c_2(x_S), c_3(x_S)]$ in Algorithm 2, and this ensemble method is called a *Qboost-Plus* classifier [2].

C. Benchmarking Qboost and Qboost-Plus for the Two-Class Classification

We run our experiment in several scenarios for the two-label dataset of the Indian Pine HSI by using the *DTC*, *SVM*, *Qboost*, *Qboost-Plus*, and *Adaboost* classifier. These scenarios are as follows.

1) *DTC* for the two-label dataset of the Indian HSI.
2) *SVM* for the two-label dataset of the Indian HSI.
3) *Qboost* with 30 weak classifiers for the two-label dataset of the Indian HSI; the weak classifiers are the DT classifiers with the depth three.
4) *Qboost-Plus* for the two-label dataset of the Indian HSI; the weak classifiers are a DTC, an SVM, and a Qboost classifier.
5) *Adaboost* with 30 weak classifiers for the two-label dataset of the Indian HSI; the weak classifiers are the decision stump classifiers.

TABLE III
CLASSIFICATION ACCURACY OF THE *DTC*, *SVM*, *QBOOST*, *QBOOST-PLUS*, AND *ADABOOST* FOR THE TWO-LABEL OF THE INDIAN PINE HSI; $\{i, j\}$ REPRESENTS THE TWO-LABELS, W.G., $\{1, 2\} \rightarrow$ *ALFALFA AND CORN-NOTILL* (SEE FIG. 1)

Binary Classifier Accuracy					
Classes	DTC	SVM	Qboost	Qboost-Plus	Adaboost
$\{1, 2\}$	0.99	0.99	0.99	0.99	0.99
$\{2, 3\}$	0.89	0.83	0.64	**0.85**	0.84
$\{3, 4\}$	0.88	0.92	0.83	**0.92**	0.90
$\{4, 5\}$	0.95	0.98	0.95	**0.98**	0.96
$\{5, 6\}$	0.99	0.99	0.98	**0.99**	0.98
$\{6, 7\}$	1.00	1.00	1.00	1.00	1.00
$\{7, 8\}$	0.95	0.99	0.99	0.99	0.99
$\{8, 9\}$	1.00	1.00	1.00	1.00	1.00
$\{9, 10\}$	1.00	0.99	0.99	0.99	0.99
$\{10, 11\}$	0.75	0.78	0.72	0.75	**0.78**
$\{11, 12\}$	0.83	0.86	0.83	**0.86**	0.84
$\{12, 13\}$	1.00	1.00	1.00	1.00	1.00
$\{13, 14\}$	0.99	0.99	0.99	0.99	0.99
$\{14, 15\}$	0.85	0.90	0.87	**0.90**	0.88
$\{15, 16\}$	0.99	0.99	0.99	0.99	0.99

By a **Bold** font, we noted the highest accuracy value of the Qboost-Plus classifier with respect to the Adaboost classifier.

All aforementioned scenarios used for benchmarking are the two-label classification of the Indian Pine HSI, and we present the classification accuracy of our experiment in Table III. We even compared the boosting algorithms, the *Qboost-Plus* and the *Adaboost* classifier. Their results demonstrate that the *Qboost-Plus* classifier performs the same as the *Adaboost* classifier and even better in some instances.

In this part, we selected the most highly informative band of the Indian Pine HSI by using our QUBO-based band subset selection method. Furthermore, we leveraged these selected bands to benchmark our *Qboost* and *Qboost-plus* algorithms with respect to the classical classifiers. Our quantum classifiers clearly outperform the conventional classifiers for most of the binary instances of the Indian pine HSI.

VII. NOVEL MULTILABEL CLASSIFIER FOR THE INDIAN PINE HSI ON A D-WAVE QA

In the prior section, we exhibited that our quantum binary classifiers (*Qboost* and *QboostPlus*) classify the two-label of the Indian Pine HSI with high accuracy due to the binary output of a D-Wave QA. However, the Indian Pine HSI has 16 classes, and the quantum binary classifiers are needed to extend for the multilabel classification. Hence, we propose a novel technique for the multilabel classification via an ECOC, and namely, we leverage an ECOC technique to classify the multilabel of the Indian Pine HSI when using our binary quantum classifiers [15], [16], [23].

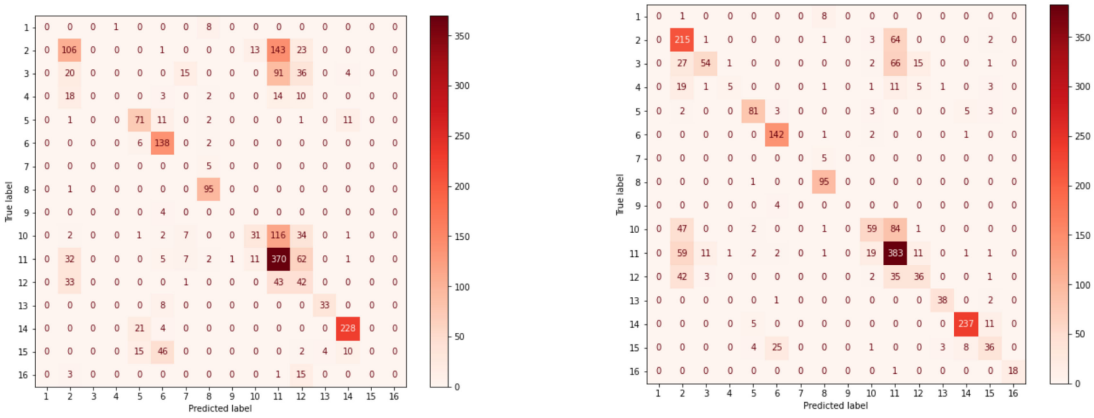

(a) (b)

Fig. 3. Confusion matrix for the $l = 16$ labels of the Indian Pine HSI. (a) *Qboost-Plus* classifier via the ECOC technique. (b) *Adaboost* classifier via the ECOC technique.

Algorithm 3: A Multilabel Classifier by Using Quantum Binary Classifiers Via an ECOC.

1: **INPUT:** Training bands:
$(\mathbf{x}, \mathbf{y}) = (x_1, y_1), \ldots, (x_S, y_S)$; $\triangleright x_S$ represents the three selected bands for a given class y_S (see Table I).
$\mathbf{y} \in \{1, 2, \ldots, 16\}^S$;
$\triangleright$ $\mathbf{y}$ represents $l = 16$ distinct labels of the Indian Pine HSI, and S is a size of the training dataset.
2: **OUTPUT:** Quantum binary classifiers:
$C_b = \{C_1, C_2, \ldots, C_{24}\}$.
3: **CODING MATRIX**:
4: Assign $b = 24$ codewords to each class ($b > \log_2\ l$), and generate l by b coding matrix M for $l = 16$ distinct labels (see Table IV).
5: Construct S by b coding matrix M' for training classes $\mathbf{y}$.
6: **TRAINING**:
7: **for** $i \leftarrow 1, \ldots, b$ **do**
8: Construct two sets, G_i and $\overline{G}_i$. G_i consists of all labels for which $M'[:, i] == 1$, and $\overline{G}_i$ is the complement set.
9: Fit a quantum binary classifier C_i to distinguish G_i from $\overline{G}_i$ by using Algorithm 2.
10: **end for**
11: **TESTING:**
12: Given an unlabeled data x_t.
13: Evaluate the trained quantum binary classifiers $C_b(x_t) = \{C_1(x_t), C_2(x_t), \ldots, C_{24}(x_t)\}$ by employing the step 17 of Algorithm 2.
14: Compute an Euclidean/Hamming distance:
$d_j = d(C_b(x_t), M[j, :]), \quad j = 1, 2, \ldots, l.$
15: **return** $\text{argmin}_j d_j$; $\triangleright$codewords (a label) for the unlabeled data x_t.
16: **STOP ALGORITHM.**

TABLE IV
EXAMPLE OF THE CODING MATRIX M FOR THE ALL $l = 16$ LABELS OF THE INDIAN PINE HSI GENERATED RANDOMLY, AND EACH CLASS IS CHARACTERIZED BY $b = 24$ CODEWORDS

Classes	A coding matrix M with $l \times b$ elements.												
1	1	1	0	1	0	1	0	0	0	0	1	...	1
2	0	1	1	0	1	0	0	0	1	1	1	...	0
⋮	⋮	⋮	⋮	⋮	⋮	⋮	⋮	⋮	⋮	⋮	⋮	...	⋮
16	0	1	0	0	1	1	1	1	1	0	1	...	1

A. ECOC Technique (see Algorithm 3 for a Detailed Procedure).

1) *Coding matrix:* We assign unique b-bits (codewords) to each class of the Indian Pine HSI such that $b > \log_2\ ^{\sim}l$ where $l = 16$ is a number of classes; the classes are represented by a so-called coding matrix $M \in \{0, 1\}^{l \times b}$ (see Table IV), and $M' \in \{0, 1\}^{S \times b}$ for a training dataset with size S. In our case, each class is represented by $b = 24$ codewords generated randomly.
2) *Training:* We train each column of the coding matrix M' by quantum binary classifiers $C_b = \{C_1, C_2, \ldots, C_{24}\}$.
3) *Testing:* For an unlabeled input x_t, we evaluate $C_b(x_t) = \{C_1(x_t), C_2(x_t), \ldots, C_{24}(x_t)\}$, and then, we assign $C_b(x_t)$ to the closest codewords in the coding matrix M by using an Euclidean/Hamming distance.

B. Benchmarking Qboost and Qboost-Plus for the Multilabel Classification

We run our experiment for the multilabel of the Indian Pine HSI via the ECOC by using the *DTC*, *SVM*, *Qboost*, *Qboost-Plus*, and *Adaboost* classifier. Furthermore, we presented the classification accuracy of our experiment in Table V. We compared also the classification accuracy and the confusion matrix of the *Qboost-Plus* with one of the *Adaboost* classifier (see Fig. 3). Their results again demonstrate that the *Qboost-Plus* classifier

TABLE V
CLASSIFICATION ACCURACY OF THE *DTC*, *SVM*, *QBOOST* CLASSIFIER, *QBOOST-PLUS* CLASSIFIER, AND *ADABOOST* CLASSIFIER FOR THE ALL 16 LABELS OF THE INDIAN PINE HSI; $\{1, 2, \ldots, 16\}$ REPRESENTS THE ALL 16 LABELS (SEE FIG. 1)

A multi-label classifier accuracy					
Classes	DTC	SVM	Qboost	Qboost-Plus	Adaboost
$\{1, 2, \ldots, 16\}$	0.82	0.72	0.67	**0.77**	0.64

By a **Bold** font, we noted the highest accuracy value of the Qboost-Plus classifier with respect to the Adaboost classifier.

beats the *Adaboost* classifier when we leverage the ECOC technique for a multilabel classification case. More importantly, we provided a novel multilabel classifier via the ECOC technique when applying a quantum computing device yielding binary outputs.

VIII. DISCUSSION AND CONCLUSION

In the first part of this article, we used an MI-based band subset selection technique as a global optimization approach for a real-world problem of the Indian Pine hyperspectral dataset on a D-Wave QA. We first mapped this MI-based band subset selection problem to a QUBO-based band subset selection problem. Then, we benchmarked and assessed the performance of a D-Wave QA compared to a conventional annealer. We demonstrated that the D-Wave QA correctly selects highly informative bands competitive to a conventional annealer. To prove that our D-Wave QA selected the best bands for each class, we classified all 16 classes based on their three highly informative bands by applying a DTC and a SVM classifier. Their classification results exhibit that the selected bands are the highly informative ones. Besides, the feature selection method saves storage space and reduces the computational load for the training process.

In the second part of our article, we first tested a binary classification for the Indian Pine HSI due to the binary output of our D-Wave QA. We proposed to employ two binary quantum classifiers, Qboost and Qboost-Plus, to our two-label dataset. Second, we provided an ECOC for the multilabel classification of the Indian Pine HSI when applying our binary quantum classifiers. Here, the classes are characterized by the bands selected during the first part of our study. We benchmarked these binary quantum classifiers and the novel multilabel classifier in comparison to conventional classifiers that are a DTC, a SVM classifier, and an Adaboost classifier. Our binary quantum classifiers and our novel multilabel classifier even outperform these conventional classifiers for most instances of the two- and multilabel dataset.

In the end, we realized how to leverage a quantum annealing device to extract knowledge and support real-world optimization problems in comparison to conventional machine learning techniques. In addition, we conceived strategies for formulating and embedding real-world problems to the topology of a D-Wave machine.

We must note, however, that our method is not intended to compete with a conventional method, but we intended to find a proper dataset in Earth observation to evaluate an existing quantum algorithm on a D-Wave QA or the future quantum computers since the choice and the size of a dataset play a vital role in quantum computers.

In terms of a future work, we will design a hybrid quantum-classical network for Earth observation datasets, which exploits both quantum computers (a QA and gate-based quantum computer) and a conventional computer. Such a hybrid network will be independent of the choice and size of datasets.

ACKNOWLEDGMENT

The authors would like to thank G. Schwarz (DLR, Oberpfaffenhofen) for his valuable comments and contributions for enhancing a quality of this article.

REFERENCES

[1] E. Farhi, J. Goldstone, S. Gutmann, and M. Sipser, "Quantum computation by adiabatic evolution," *arXiv:0001106*, Jan. 2000. [Online]. Available: https://arxiv.org/abs/quant-ph/0001106

[2] *A D-Wave Quantum Annealer*, 2021. [Online]. Available: https://cloud.dwavesys.com/leap

[3] V. S. Denchev *et al.*, "What is the computational value of finite-range tunneling?" *Phys. Rev. X*, vol. 6, Aug. 2016, Art. no. 031015. [Online]. Available: https://link.aps.org/doi/10.1103/PhysRevX.6.031015

[4] E. Farhi, J. Goldstone, S. Gutmann, J. Lapan, A. Lundgren, and D. Preda, "A quantum adiabatic evolution algorithm applied to random instances of an NP-complete problem," *Science*, vol. 292, no. 5516, pp. 472–475, 2001. [Online]. Available: https://science.sciencemag.org/content/292/5516/472

[5] T. Stollenwerk *et al.*, "Quantum annealing applied to de-conflicting optimal trajectories for air traffic management," *IEEE Trans. Intell. Transp. Syst.*, vol. 21, no. 1, pp. 285–297, Jan. 2020.

[6] E. Rieffel, D. Venturelli, B. O'Gorman, M. Do, E. Prystay, and V. Smelyanskiy, "A case study in programming a quantum annealer for hard operational planning problems," *Quantum Inf. Process.*, vol. 14, pp. 1–36, 2015.

[7] F. Melgani and L. Bruzzone, "Classification of hyperspectral remote sensing images with support vector machines," *IEEE Trans. Geosci. Remote Sens.*, vol. 42, no. 8, pp. 1778–1790, Aug. 2004.

[8] S. Prasad and L. M. Bruce, "Limitations of principal components analysis for hyperspectral target recognition," *IEEE Geosci. Remote Sens. Lett.*, vol. 5, no. 4, pp. 625–629, Oct. 2008.

[9] B. Guo, S. R. Gunn, R. I. Damper, and J. D. B. Nelson, "Band selection for hyperspectral image classification using mutual information," *IEEE Geosci. Remote Sens. Lett.*, vol. 3, no. 4, pp. 522–526, Oct. 2006.

[10] S. Sarmah and S. K. Kalita, "Mutual information-based hierarchical band selection approach for hyperspectral images," in *Advances in Electronics, Communication and Computing*, A. Kalam, S. Das, and K. Sharma, Eds. Singapore: Springer, 2018, pp. 755–763.

[11] X. V. Nguyen, J. Chan, S. Romano, and J. Bailey, "Effective global approaches for mutual information based feature selection," in *Proc. 20th ACM SIGKDD Int. Conf. Knowl. Discov. Data Mining*, 2014, pp. 512–521. [Online]. Available: https://doi.org/10.1145/2623330.2623611

[12] N. X. Vinh, S. Zhou, J. Chan, and J. Bailey, "Can high-order dependencies improve mutual information based feature selection?" *Pattern Recognit.*, vol. 53, pp. 46–58, 2016. [Online]. Available: https://www.sciencedirect.com/science/article/pii/S0031320315004276

[13] H. Neven, V. S. Denchev, G. Rose, and W. G. Macready, "Qboost: Large scale classifier training with adiabatic quantum optimization," in *Proc. Asian Conf. Mach. Learn.*, Nov. 2012, vol. 25, pp. 333–348. [Online]. Available: http://proceedings.mlr.press/v25/neven12.html

[14] V. S. Denchev, N. Ding, S. V. N. Vishwanathan, and H. Neven, "Robust classification with adiabatic quantum optimization," *arXiv:1205.1148*, May 2012. [Online]. Available: https://arxiv.org/abs/1205.1148

[15] T. G. Dietterich and G. Bakiri, "Solving multiclass learning problems via error-correcting output codes," *J. Artif. Int. Res.*, vol. 2, no. 1, pp. 263–286, Jan. 1995.

[16] A. Radoi and M. Datcu, "Multilabel annotation of multispectral remote sensing images using error-correcting output codes and most ambiguous examples," *IEEE J. Sel. Topics Appl. Earth Observ. Remote Sens.*, vol. 12, no. 7, pp. 2121–2134, Jul. 2019.
[17] *Airborne visible/infrared Imaging Spectrometer (AVIRIS)*, 2021. [Online]. Available: https://aviris.jpl.nasa.gov/
[18] S. Barnett, Ed., *Quantum Information*. Oxford, U.K.: Oxford Univ. Press, 2009.
[19] K. Boothby, P. Bunyk, J. Raymond, and A. Roy, "Next-generation topology of D-wave quantum processors," *arXiv:2003.00133,* Feb. 2020. [Online]. Available: https://arxiv.org/abs/2003.00133
[20] Y. Freund and R. E. Schapire, "A decision-theoretic generalization of online learning and an application to boosting," *J. Comput. Syst. Sci.*, vol. 55, no. 1, pp. 119–139, 1997. [Online]. Available: https://www.sciencedirect.com/science/article/pii/S002200009791504X
[21] T. Hastie, S. Rosset, J. Zhu, and H. Zou, "Multi-class adaboost," *Statist. Interface*, vol. 2, no. 3, pp. 349–360, 2009.
[22] E. Boyda, S. Basu, S. Ganguly, A. Michaelis, S. Mukhopadhyay, and R. R. Nemani, "Deploying a quantum annealing processor to detect tree cover in aerial imagery of California," *PLOS One*, vol. 12, no. 2, pp. 1–22, Feb. 2017. [Online]. Available: https://doi.org/10.1371/journal.pone.0172505
[23] A. Berger, "Error-correcting output coding for text classification," in *Proc. IJCAI-99 Workshop Mach. Learn. Inf. Filtering*, Jul. 2001.

Soronzonbold Otgonbaatar received the B.Sc. degree from the National University of Mongolia, Ulaanbaator, Mongolia, and the M.Sc. degree in theoretical physics from the University of Siegen, Siegen, Germany, in 2014 and 2016, respectively. He is currently working toward the Ph.D. degree with German Aerospace Center, Wessling, Germany.

His research interests include computational science, artificial intelligence (i.e., machine learning), quantum computing and algorithms, and quantum machine learning with practical applications in remote sensing data.

Mihai Datcu (Fellow, IEEE) received the M.S. and Ph.D. degrees in electronics and telecommunications from the University Politehnica of Bucharest (UPB), Bucharest, Romania, in 1978 and 1986, respectively, and the habilitation a Diriger Des Recherches degree in computer science from the University Louis Pasteur, Strasbourg, France, in 1999.

Since 1981, he has been a Professor with the Department of Applied Electronics and Information Engineering, Faculty of Electronics, Telecommunications and Information Technology, UPB. Since 1993, he has been a Scientist with the German Aerospace Center (DLR), Wessling, Germany. He has held Visiting Professor appointments with the University of Oviedo, Spain, the University Louis Pasteur and the International Space University, both in Strasbourg, France, the University of Siegen, Germany, the University of Innsbruck, Austria, the University of Alcala, Spain, the University Tor Vergata, Rome, Italy, the University of Trento, Italy, the Unicamp, Campinas, Brazil, the China Academy of Science, Shenyang, China, the Universidad Pontificia de Salamanca, Campus de Madrid, Spain, the University of Camerino, Italy, and the Swiss Center for Scientific Computing, Manno, Switzerland. From 1992 to 2002, he had an Invited Professor Assignment with the Swiss Federal Institute of Technology, Switzerland. Since 2001, he had been initiating and leading the Competence Center on Information Extraction and Image Understanding for Earth Observation, Paris Institute of Technology, ParisTech, France, a collaboration of DLR with the French Space Agency. He has been a Professor holder of the DLR-CNES Chair with ParisTech. He has initiated the European frame of projects for image information mining and is involved in research programs for information extraction, data mining and knowledge discovery, and data science with the ESA, NASA, and in a variety of national and European projects. He is the Director of the Research Center for Spatial Information, UPB. He is a Senior Scientist and the Data Intelligence and Knowledge Discovery Research Group Leader with the Remote Sensing Technology Institute, DLR, and a delegate with the DLR-ONERA Joint Virtual Center for AI in Aerospace. He is a member of the ESA Working Group Big Data from Space and Visiting Professor with ESA's Phi-Lab. His research interests include explainable and physics-aware artificial intelligence, smart radar sensors design, and quantum machine learning with applications in Earth observation.

Dr. Datcu was the recipient of the National Order of Merit with the rank of Knight, for outstanding international research results, awarded by the President of Romania, in 2008, and the Romanian Academy Prize Traian Vuia for the development of the SAADI image analysis system and his activity in image processing in 1987. He was awarded the Chaire D'excellence Internationale Blaise Pascal 2017 for data science in Earth observation and the 2018 Ad Astra Award for Excellence in Science. He has served as a Coorganizer for international conferences and workshops and as a Guest Editor for the IEEE and other journals. He is representative of Romanian in the Earth Observation Program Board.